

Systematic generation of higher-order solitons and breathers of the Hirota equation on different backgrounds

Stanko N. Nikolić · Najdan B. Aleksić ·
Omar A. Ashour · Milivoj R. Belić · Siu A. Chin

Received: 1 February 2017 / Accepted: 20 April 2017 / Published online: 8 May 2017
© Springer Science+Business Media Dordrecht 2017

Abstract We investigate the systematic generation of higher-order solitons and breathers of the Hirota equation on different backgrounds. The Darboux transformation is used to construct proper initial conditions for dynamical generation of high-intensity solitons and breathers of different orders on a uniform background. We provide expressions for the Lax pair generating functions and the procedure for calculating higher-order solutions when Jacobi elliptic functions are the background seed solutions of the Hirota equation. We confirm that the peak height of each soliton or breather in the nonlinear Darboux superposition adds linearly, to form the intensity maximum of the final solution.

Keywords Hirota equation · Darboux transformation · Higher-order solitons · Breathers and rogue waves

S. N. Nikolić (✉) · N. B. Aleksić · O. A. Ashour ·
M. R. Belić
Science Program, Texas A&M University at Qatar,
P.O. Box 23874 Doha, Qatar
e-mail: stankon@ipb.ac.rs

S. N. Nikolić · N. B. Aleksić
Institute of Physics Belgrade, University of Belgrade,
Pregrevica 118, Belgrade 11080, Serbia

O. A. Ashour · S. A. Chin
Department of Physics and Astronomy, Texas A&M University,
College Station, TX 77843, USA

1 Introduction

In this work, we study the solitons and breathers of the Hirota equation (HE) [1–3]

$$i \frac{\partial \psi}{\partial x} + \frac{1}{2} \frac{\partial^2 \psi}{\partial t^2} + |\psi|^2 \psi - i\alpha \left(\frac{\partial^3 \psi}{\partial t^3} + 6|\psi|^2 \frac{\partial \psi}{\partial t} \right) = 0 \quad (1.1)$$

on various backgrounds. Here, x and t are the retarded time in the moving frame and the transverse spatial variable, respectively, while ψ denotes the slowly varying wave envelope.

The fundamental solutions of HE are of great importance in many fields dealing with nonlinear propagating waves, ranging from oceanography to fiber-optics [4]. HE contains only one real parameter α , related to the transverse velocity of the wave. Setting $\alpha = 0$ reduces HE to the nonlinear Schrödinger equation (NLSE) [5–8]. The necessity of extending the NLSE to the HE and other higher-order members of the NLS hierarchy of equations arises from the need to understand propagation of ultrashort pulses through optical fibers [9, 10]. A more accurate description of the real physical systems requires additional terms, to account for self-steepening, self-frequency shift, and third-order dispersion [11–15]. It was shown that these third-order terms are of significant importance in pulse-deforming phenomena [16] and supercontinuum generation [17].

In this work, we show that the solitons and breathers of high intensity can be *dynamically* generated on zero and constant backgrounds by a direct numerical inte-

gration of an initial wave function extracted from the Darboux transformation (DT), with appropriate boundary conditions. We also find new Hirota solutions, derived by DT on an elliptic background. In all the cases, we demonstrate that the peak height formula [(PHF—Eq. (4.1)] gives the correct peak value of a higher-order solution of HE, as a linear sum of peak heights of its DT constituents [18].

Solitons, breathers and rational solutions of HE have been previously studied using DT in Refs. [2, 19–22]. Additional interest in NLSE and Hirota breathers arises from their relationship with the rogue waves (RWs) [23–27] that can be modeled by higher-order breathers concatenated from the first-order ones via DT iterations [24, 27–29]. An interesting finding in Hirota [30] and quintic NLSE [31] is the breather-to-soliton conversion, obtained for specific values of the breather eigenvalues—a feature not possible in the ordinary cubic NLSE. The study of NLSE breathers on a Jacobi elliptic function (JEF, see [32]) background was previously done in Refs. [33, 34]. A recent discovery of an infinite hierarchy of extended nonlinear Schrödinger equations [35–38] has also revealed that they may only have dnoidal and cnoidal backgrounds in their solutions. To the extent that HE can better describe light propagation in an optical fiber, this work should also contribute to a better understanding of optical RW generation.

The paper is organized as follows: In Sect. 2, we analyze the basic Hirota solutions and show the usefulness of DT for numerical simulations. In Sect. 3, we provide a derivation of the Lax pair generating functions and higher-order solutions when cnoidal and dnoidal functions are taken as seed solutions in DT. In Sect. 4, the PHF for HE is presented. In Sect. 5, we present analytical and numerical results concerning higher-order solitons and breathers on different backgrounds, utilizing the periodicity of ABs and breather-to-soliton conversion. In Sect. 6, we summarize the findings and importance of our results. The general DT scheme is provided in “Appendix.”

2 Solitons and breathers of the Hirota equation

Darboux transformation can be used to obtain higher-order soliton/breather and rogue wave solutions of the Hirota equation on different backgrounds. The key steps in obtaining these nonlinear structures *dynam-*

ically, for discretized x and t intervals, are: 1. use DT to calculate the initial wave function at a particular value of the propagation variable $x = x_0$, i.e., to find $\psi(x_0, t)$, 2. analyze the wave function values at the edges of the t -interval in order to pick appropriate boundary conditions, and 3. apply a convenient numerical algorithm to calculate the wave function over the entire xt -grid (in this case, the fourth-order Runge–Kutta method).

To numerically generate higher-order solitons, we calculate the initial wave function from a zero seed: $\psi_0 = 0$. The appropriate boundary condition can be found from the first-order DT solution, characterized by a pure imaginary eigenvalue $\lambda = i\nu$ (without loss of generality, we can assume zero shifts along the x and t axes),

$$\psi(x, t) = \frac{2\nu e^{2i\nu^2 x}}{\cosh[2\nu(t + 4\alpha\nu^2 x)]}. \quad (2.1)$$

From (2.1), it follows that the first-order soliton has a single peak with the amplitude $|\psi(0, 0)| = 2\nu$, and its intensity decays exponentially, following the cosh function. Consequently, the Neumann boundary condition $\frac{\partial\psi}{\partial t} = 0$ can be used in numerical evaluations of higher-order Hirota solitons. It should be noted that the Hirota coefficient α appears only in the denominator, giving a tilt to the soliton propagation.

A higher-order Akhmediev breather (AB) of HE is constructed by DT when a plane-wave seed, $\psi_0 = e^{ix}$, is utilized. The first-order AB is given by [19]

$$\psi(x, t) = \left[\frac{2(1 - 2a) \cosh(\beta x) + i\beta \sinh(\beta x)}{\cosh(\beta x) - \sqrt{2a} \cos[\omega(t + vx)]} - 1 \right] e^{ix}, \quad (2.2)$$

where a is an arbitrary parameter in the range $0 < a < 1/2$. The frequency ω , the growth factor β , and the parameter v determining the tilt of the breather in the xt -plane are given solely in terms of a :

$$\omega = 2\sqrt{1 - 2a}, \quad \beta = \omega\sqrt{2a}, \quad v = 2\alpha(1 + 4a). \quad (2.3)$$

The difference between NLSE and Hirota breathers originates only from the parameter v . NLSE solutions are obtained when $v = 0$ ($\alpha = 0$).

From Eq. (2.2), one can see that Hirota’s AB is periodic along t -axis, with the period

$$L = \frac{2\pi}{\omega} = \frac{\pi}{\sqrt{1-2a}}. \tag{2.4}$$

Consequently, in contrast to solitons, periodic boundary conditions are required for dynamical generation of higher-order ABs. Briefly, one assumes that each of N eigenvalues is purely imaginary $\lambda_j = i v_j$. The parameter a_j of each breather constituent is connected to the imaginary part of its eigenvalue via the relation

$$v_j = \sqrt{2a_j}. \tag{2.5}$$

Due to periodicity, it is natural to choose higher-order breathers that retain the same periodic length L of the first-order breather, having $\omega_j = j\omega$ ($a_1 \equiv a, \omega_1 \equiv \omega$). From Eqs. (2.3) to (2.5), it follows

$$\lambda_j = i \sqrt{2 \left(j^2 a - \frac{j^2 - 1}{2} \right)}. \tag{2.6}$$

If, for any j , ω_j is not an integer multiple of ω , then the periodicity of the original breather is destroyed. For more details, see [18]. The procedure for generating higher-order ABs is to take an initial a , calculate other eigenvalues according to Eq. (2.6), and apply the DT.

3 New solutions of the Hirota equation on dnoidal/cnoidal backgrounds

In recent articles [35,36], new exact solutions of HE that include JEFs are presented:

$$\psi_{\text{dn}}(x, t) = c e^{i\phi x} \text{dn}(ct + vx, m), \tag{3.1}$$

$$\psi_{\text{cn}}(x, t) = \frac{c}{\sqrt{2}} \sqrt{s+1} e^{i\phi x} \cdot \text{cn} \left(\sqrt{s} ct + \sqrt{s} vx, m = \frac{1}{2} + \frac{1}{2s} \right). \tag{3.2}$$

Here, m is the elliptic modulus squared, c, s, ϕ are constants, and v is the speed of the wave that depends on α . By setting $c = 2v$ and $m = 1$, we reproduce the soliton solution of Eq. (2.1). Any of these functions may be used as a seed for the Darboux transformation. This motivated us to examine how higher-order solutions can be obtained on dnoidal/cnoidal backgrounds. All results in this section are derived using the general Darboux transformation scheme for Hirota equation given in ‘‘Appendix.’’

3.1 Derivation of the DT Lax pair generating

functions and higher-order solutions for $\psi_0 = \psi_{\text{dn}}$

Here the seed function ψ_0 is given by Eq. (3.1) with $\phi = (1 - \frac{m}{2})c^2$ and $v = (2 - m)\alpha c^3$ [35]. The Lax pair equations consist of a system of four coupled linear differential equations for $r_t, s_t, r_x,$ and s_x . Here, the subscripts stand for partial derivatives. To solve these equations, we introduce the traveling variable

$$u = ct + xv \tag{3.3}$$

and continue the analysis with x and u . Now, the t -derivatives are replaced by the u -derivatives: $\frac{\partial \psi}{\partial t} = c^2 e^{i\phi x} \frac{\partial \text{dn}(u)}{\partial u}$ and $\frac{\partial^2 \psi}{\partial t^2} = c^3 e^{i\phi x} \frac{\partial^2 \text{dn}(u)}{\partial u^2}$. We take the ansatz:

$$\begin{aligned} r(x, u) &= g(x, u) e^{-i\phi x/2} \text{ and} \\ s(x, u) &= h(x, u) e^{+i\phi x/2}. \end{aligned} \tag{3.4}$$

The matrix elements of U and V from Eq. (7.4) in ‘‘Appendix’’ can be calculated by substituting ψ_0 into Eq. (7.5). From Eq. (7.4), the u -evolutions are obtained

$$g_u = i \frac{\lambda}{c} g + i \cdot \text{dn}(u) h, \tag{3.5}$$

$$h_u = i \cdot \text{dn}(u) g - i \frac{\lambda}{c} h. \tag{3.6}$$

The equations for the x -derivative are a bit more complicated, but actually not needed for numerical calculations. It is only necessary to obtain the x -derivative at $u = 0$, to initiate the numerical integration of r and s . Evolution along the x -axis at $u = 0$ follows from Eq. (7.3)

$$g_x = i A g + i B h, \tag{3.7}$$

$$h_x = i B g - i A h, \tag{3.8}$$

where constants A and B are

$$A = \left(\lambda^2 - \frac{m c^2}{4} \right) (1 - 4\alpha \lambda), \tag{3.9}$$

$$B = c \lambda (1 - 4\alpha \lambda). \tag{3.10}$$

By differentiating and combining Eqs. (3.7) and (3.8) one obtains:

$$g_{xx} = -(A^2 + B^2) g \tag{3.11}$$

and

$$h_{xx} = -(A^2 + B^2) h. \tag{3.12}$$

Thus, the exact solution for g or h is $h(x, u = 0) = C_1 e^{i\kappa\lambda x} + C_2 e^{-i\kappa\lambda x}$. Here, $\kappa = \frac{\sqrt{A^2+B^2}}{\lambda}$, while C_1 and C_2 are arbitrary constants. We can embed the phase shift of $\pi/4$ into $h(x, u = 0)$, to center the solution at the origin. Next, we take $C_1 = e^{-i\pi/4-i\chi}$ and $C_2 = e^{+i\pi/4+i\chi}$. Therefore: $h(x, u = 0) = 2 \cos(-\chi + \kappa\lambda x - \pi/4)$. If we substitute $h(x, u = 0)$ in (3.8), we will get the solution $g(x, u = 0) = 2i \sin(-\chi + \kappa\lambda x - \pi/4 + \varphi)$. The idea is to make the solutions for g and h symmetrical and in agreement with the published articles [27,28,33]. We can choose $-\chi + \varphi = +\chi$, and therefore $\chi = \frac{1}{2}\varphi = \frac{1}{2} \arccos \frac{\kappa\lambda}{B}$. The solution for g is $g(x, u = 0) = 2i \sin(+\chi + \kappa\lambda x - \pi/4)$.

Now, we go back to the Lax pair generating functions, introducing N eigenvalues and x -shifts (t -axis shifts are ignored since they provide negligible advance in the understanding, alongside with numerical complications). The quantities κ and χ are labeled with the j index. Hence, the Lax pair generating functions for eigenvalue λ_j and shift x_{0j} ($1 \leq j \leq n$) are:

$$r_{1j}(x, u = 0) = 2i e^{-i\phi x/2} \sin[+\chi_j + \kappa_j \lambda_j (x - x_{0j}) - \pi/4] \tag{3.13}$$

$$s_{1j}(x, u = 0) = 2e^{+i\phi x/2} \cos[-\chi_j + \kappa_j \lambda_j (x - x_{0j}) - \pi/4], \tag{3.14}$$

where

$$\kappa_j = (1 - 4\alpha\lambda_j) \sqrt{c^2 + \left(\lambda_j - \frac{mc^2}{4\lambda_j}\right)^2} \tag{3.15}$$

$$\chi_j = \frac{1}{2} \arccos \frac{\kappa_j}{c(1 - 4\alpha\lambda_j)}. \tag{3.16}$$

The remaining task is to find the $r_{1,j}$ and $s_{1,j}$ functions for any u . The evolution equations are given by expressions (3.5) and (3.6). We can solve them only numerically, for instance using the fourth-order Runge–Kutta method. We write $u = ct + xv = 0$ and for a given x , we find $t = -\frac{v}{c}x$. We start from this t value and numerically evolve $du = cdt$ (in both directions) to find $r_{1,j}(x, u)$ and $s_{1,j}(x, u)$. Next, we shift these values from the (x, u) to the (x, t) frame, to get all values on the grid: $r(x, t)$ and $s(x, t)$. Finally, by employing the well-known recursive relations in Eq. (7.2) and iterative relations in Eq. (7.1), the N th-order

solution, $\psi_N(x, t)$, can be calculated. In the special case of $\alpha = 0$ and $c = 1$, the Hirota Lax pair generating functions and the final N th-order wave function are equivalent to the NLSE solutions described in Section 2.2 of [33].

3.2 Derivation of the DT Lax pair generating

functions and higher-order solutions for $\psi_0 = \psi_{cn}$

The analysis is analogous to the previous case. The seed function ψ_0 is given by Eq. (3.2), where $\phi = \frac{1}{2}c^2$ and $v = \alpha c^3$. The substitution

$$u = \sqrt{s}(ct + xv) \tag{3.17}$$

gives $\frac{\partial \psi}{\partial t} = c^2 \sqrt{\frac{s(s+1)}{2}} e^{i\phi x} \frac{\partial \text{cn}(u)}{\partial u}$ and $\frac{\partial^2 \psi}{\partial t^2} = c^3 s \sqrt{\frac{s+1}{2}} e^{i\phi x} \frac{\partial^2 \text{cn}(u)}{\partial u^2}$. The ansatz is now:

$$\begin{aligned} r(x, u) &= g(x, u) e^{-i\phi x/2} \text{ and} \\ s(x, u) &= h(x, u) e^{+i\phi x/2}. \end{aligned} \tag{3.18}$$

The evolution along u -axis (from the U matrix) is

$$g_u = \frac{i\lambda}{c\sqrt{s}} g + \frac{i\sqrt{s+1}}{\sqrt{2s}} \text{cn}(u) h, \tag{3.19}$$

$$h_u = \frac{i\sqrt{s+1}}{\sqrt{2s}} \text{cn}(u) g - \frac{i\lambda}{c\sqrt{s}} h. \tag{3.20}$$

Again, we restrict further analysis only to $u = 0$. The evolution along the x -axis is:

$$g_x = iAg + iBh, \tag{3.21}$$

$$h_x = iBg - iAh, \tag{3.22}$$

where

$$A = (1 - 4\alpha\lambda) \left(\lambda^2 - \frac{1}{4}c^2s \right), \tag{3.23}$$

$$B = \frac{c\lambda\sqrt{m}}{\sqrt{2m-1}} (1 - 4\alpha\lambda). \tag{3.24}$$

By differentiating the last two equations, one gets

$$g_{xx} = -(A^2 + B^2)g, \tag{3.25}$$

$$h_{xx} = -(A^2 + B^2)h. \tag{3.26}$$

The exact solution for h is $h(x, u = 0) = C_1 e^{i\kappa\lambda x} + C_2 e^{-i\kappa\lambda x}$, with $\kappa = \frac{\sqrt{A^2+B^2}}{\lambda}$. We choose C_1 and C_2 constants as in the previous case. The final solution for Lax pair generating functions is obtained

after the complete sets of eigenvalues and x -shifts are introduced,

$$r_{1j}(x, u = 0) = 2ie^{-i\phi x/2} \sin[+\chi_j + \kappa_j \lambda_j(x - x_{0j}) - \pi/4], \tag{3.27}$$

$$s_{1j}(x, u = 0) = 2e^{+i\phi x/2} \cos[-\chi_j + \kappa_j \lambda_j(x - x_{0j}) - \pi/4], \tag{3.28}$$

where

$$\kappa_j = (1 - 4\alpha\lambda_j) \cdot \sqrt{m} \sqrt{\frac{c^2}{2m-1} + \frac{1}{m} \left(\lambda - \frac{c^2}{2m-1} \cdot \frac{1}{4\lambda} \right)^2}, \tag{3.29}$$

$$\chi_j = \frac{1}{2} \arccos \frac{\kappa_j \sqrt{2m-1}}{c\sqrt{m}(1-4\alpha\lambda_j)}. \tag{3.30}$$

The Lax pairs generating functions for both dn and cn seedings have the same form. However, parameters κ_j and χ_j differ in the two cases, so the r and s functions and the final solutions differ too. An equivalent numerical scheme, proposed in the previous subsection, can be used to calculate r and s functions for any x and u , and then over the entire xt -grid. Again, in the special case of $\alpha = 0$ and $c = \sqrt{2m-1}$, the Hirota Lax pair generating functions and the final N th-order solution are equivalent to the NLSE solutions described in Section 2.3 of [33].

4 Peak height formula for the Hirota equation

We have stated that the maximum amplitude of the N th order DT solution is just a *linear* sum of peak heights

of the individual solitons or breathers in the *nonlinear* superposition. In [34], we have proven that the peak height formula (PHF) holds regardless of the choice of the seed function in DT,

$$\psi_N(0, 0) = \psi_0(0, 0) + \sum_{n=1}^N 2v_n. \tag{4.1}$$

Again, the assumption is that all N eigenvalues are purely imaginary $\lambda_j = iv_j$ (the real part would not change the PHF). It is proven in [18] that PHF holds when the Lax pair generating functions satisfy the following equation, assuming zero x and t shifts for all eigenvalues:

$$s_{1,j}(0, 0) = ir_{1,j}(0, 0). \tag{4.2}$$

In Table 1, explicit expressions for the seed and Lax pair generating functions of HE are given. For brevity, we omit “ j ” index in N eigenvalues.

It is easy to check that the relation in Eq. (4.2) applies to all cases given in Table 1.

For the potential applications of soliton propagation in optical fibers modeled by HE, a high soliton intensity is an advantage. As explained in detail in [30], a breather can be converted to a soliton for a specific value of the real part $\Re\{\lambda_j\}$ of all eigenvalues,

$$\Re\{\lambda_j\} = \frac{1}{8\alpha}. \tag{4.3}$$

According to the PHF, this means that such a “converted” soliton (single or higher order) would have greater amplitude compared to the one obtained with zero seed, having the same set of eigenvalues.

Table 1 Seed solutions for Hirota equation and the corresponding Lax pair generating functions ($r_{1,j} \equiv r$ and $s_{1,j} \equiv s$)

| Seed function $\psi_0(x, t)$ | Lax pair generating functions | PHF |
|------------------------------|--|---|
| 0 | $r(x, t) = e^{i[\lambda t - \lambda^2(4\alpha\lambda - 1)x - \pi/4]}$ $s(x, t) = e^{-i[\lambda t - \lambda^2(4\alpha\lambda - 1)x - \pi/4]}$ | $\psi_N(0, 0) = \sum_{n=1}^N 2v_n$ |
| e^{ix} | $r(x, t) = 2ie^{-ix/2} \sin(\chi + \frac{1}{2}\kappa t + \frac{1}{2}dx - \pi/4)$ $s(x, t) = 2e^{+ix/2} \cos(-\chi + \frac{1}{2}\kappa t + \frac{1}{2}dx - \pi/4)$ | $\psi_N(0, 0) = 1 + \sum_{n=1}^N 2v_n$ |
| $\psi_{dn}(x, t)$ | $r(0, 0) = 2i \sin(+\chi - \pi/4)$ $s(0, 0) = 2 \cos(-\chi - \pi/4)$ | $\psi_N(0, 0) = c + \sum_{n=1}^N 2v_n$ |
| $\psi_{cn}(x, t)$ | $r(0, 0) = 2i \sin(+\chi - \pi/4)$ $s(0, 0) = 2 \cos(-\chi - \pi/4)$ | $\psi_N(0, 0) = c\sqrt{\frac{m}{2m-1}} + \sum_{n=1}^N 2v_n$ |

5 Numerical verification

Here we present numerical simulations of higher-order solitons and breathers on uniform and nonuniform backgrounds and introduce a simple criterion to estimate the solution peak value using the PHF.

5.1 Solutions of Hirota equation on uniform backgrounds

First, we show that the single-soliton solutions, obtained by DT (Fig. 1a) and by dynamical integration (Fig. 1b), are in excellent agreement if one chooses the Neumann boundary conditions. The maximum intensity in both figures is 7.84, in agreement with PHF ($\lambda = 1 + 0.9i$), $7.84 = (0 + 2 \cdot 0.9)^2$. The second-

order soliton is shown in Fig. 1c (DT) and 1d (direct integration). It is generated from the two single solitons, characterized by eigenvalues $\lambda_1 = 1 + 0.9i$ and $\lambda_2 = 1 + i$. The maximum intensity in this case is $14.44 = (0 + 2 \cdot 0.9 + 2 \cdot 1)^2$. The tilt in the soliton propagation in all figures mainly comes from the Hirota parameter $\alpha = 1/8$, but also from the real part of eigenvalues.

In Fig. 2, we demonstrate that higher-order breathers can numerically evolve from an initial DT wave function by applying a periodic boundary condition. First, we choose $a_1 = a = 0.464$ for the first AB in a nonlinear superposition and calculate its eigenvalue according to Eq. (2.5). As stated in Sect. 2, the second- and third-order breathers should have their frequencies exactly two and three times higher than the fre-

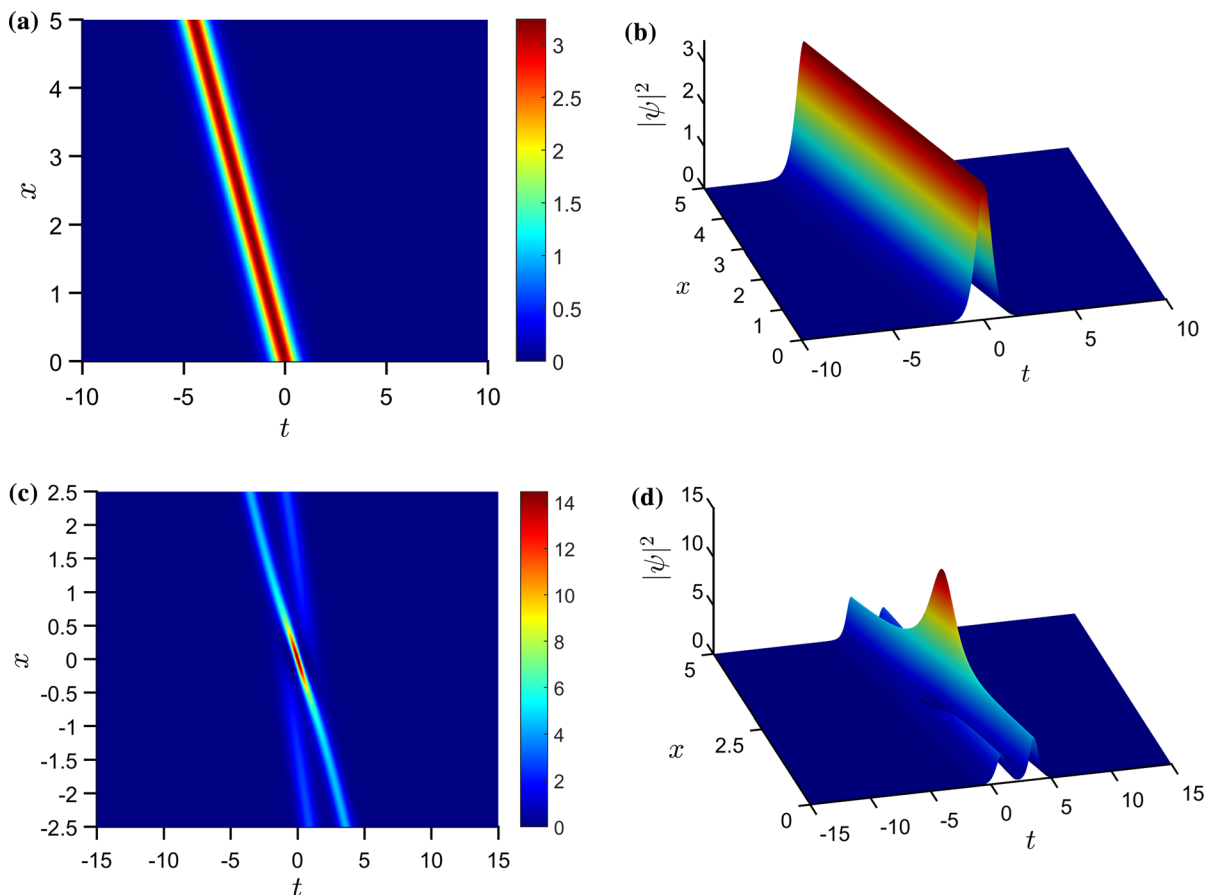


Fig. 1 Propagation of the soliton with $\alpha = 1/8$: **a** 2D intensity plot of the first-order DT solution with $\psi_0 = 0$ and $\lambda = 1 + 0.9i$; **b** numerical evolution of the initial condition taken at $x = 0$ from (a); **c** 2D intensity plot of the second-order DT solution

with $\psi_0 = 0$, $\lambda_1 = 1 + 0.9i$, and $\lambda_2 = 1 + i$; and **d** numerical evolution of the initial condition taken at $x = -2.5$ from (c). Maximum intensity value $|\psi|^2$ is 3.24 in (a) and (b), and 14.44 in (c) and (d), in agreement with PHF

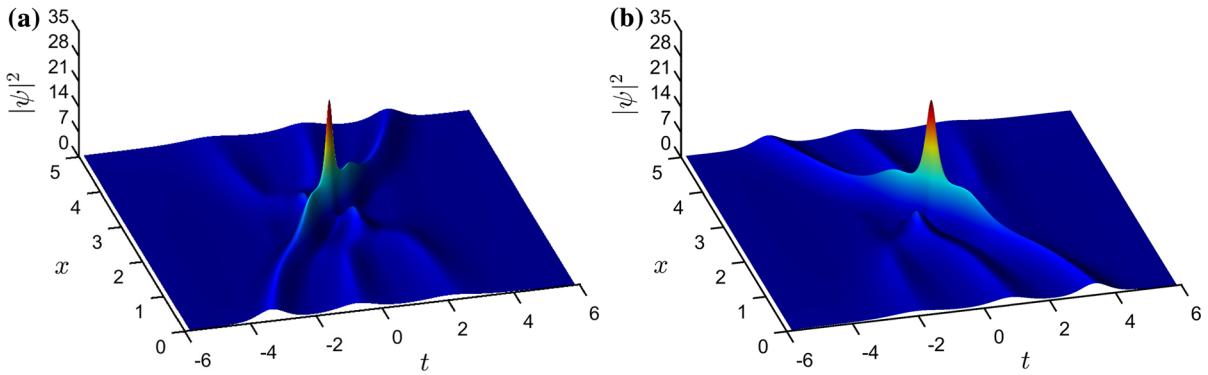


Fig. 2 Dynamically generated third-order breathers. Initial wave function is extracted from DT solution, having a plane-wave seed, at $x = -2.5$. The fundamental period is characterized by $a = 0.464$ from Eq. (2.3). Pure imaginary eigenvalues λ_j ,

with $1 \leq j \leq 3$, are calculated using Eq. (2.6). The peak intensity is $|\psi|_{\max}^2 = 33.64$, in agreement with PHF. **a** $\alpha = -0.1$, **b** $\alpha = +0.1$

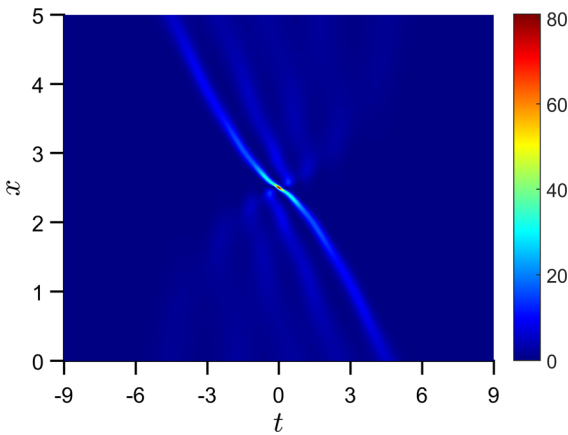


Fig. 3 2D intensity plot of dynamically generated fifth-order breather. Initial wave function is extracted from the DT solution, having a plane-wave seed, at $x = -2.5$. The fundamental period is characterized by $a = 0.485$ from Eq. (2.3). Pure imaginary eigenvalues λ_j , with $1 \leq j \leq 5$, are calculated using Eq. (2.6). The peak intensity is $|\psi|_{\max}^2 = 81$, in agreement with PHF. Hirota parameter is $\alpha = 0.1$

periodic boundary conditions. The peak intensity is $|\psi|_{\max}^2 = 81 = (1 + 2\nu_1 + 2\nu_2 + 2\nu_3 + 2\nu_4 + 2\nu_5)^2$.

Next, we utilize a breather-to-soliton conversion of HE, to further exemplify the utility of PHF. Even when the plane-wave seeding is used to generate breathers, the solitons of arbitrary orders are generated under the condition given by Eq. (4.3). One can immediately see the benefits of PHF: The “converted” soliton will have the amplitude maximum of $1 + \sum_i 2\nu_i$, instead of $\sum_i 2\nu_i$, obtained from the usual zero seed. We demonstrate this by using the same eigenvalues as in Fig. 1, but having real parts equal to $\frac{1}{8\alpha}$. The intensity peak heights of single and double converted solitons are 7.84 and 23.04, respectively, which are higher than those of the solitons of the same shape shown in Fig. 1. Real and imaginary parts of the wave function have a discontinuity at the edges of the t interval. Furthermore, $\lim_{t \rightarrow \pm\infty} |\psi|^2 = 1$ and $\lim_{t \rightarrow \pm\infty} \frac{\partial \psi}{\partial t} = 0$, so the Neumann boundary condition can still be applied in this case (Fig. 4).

quency of the first-order one. We show the third-order breather in Fig. 2a for $\alpha = -0.1$, and in Fig. 2b for $\alpha = 0.1$. The tilt and a slight stretching of the solution are determined by the parameter α solely. The PHF holds: $|\psi|_{\max}^2 = 33.64 = (1 + 2\nu_1 + 2\nu_2 + 2\nu_3)^2$.

In Fig. 3, we show a fifth-order breather, numerically obtained in the same way as the third-order breather from the previous figure. We start from $a_1 = a = 0.485$, calculate other eigenvalues accordingly (Eq. 2.6), and set the domain for numerics assuming

5.2 Solutions of Hirota equation on nonuniform backgrounds

We now switch to the solutions generated by the DT when the seed is taken from dn or cn family of JEFs, given by Eqs. (3.1) and (3.2). First, we examine if the breather-to-soliton conversion holds for nonuniform backgrounds. In Fig. 5a, b, we show the first-order converted solitons, differing only in the parameter c of Eq. (3.1). For $c = 1$, the background oscillations have

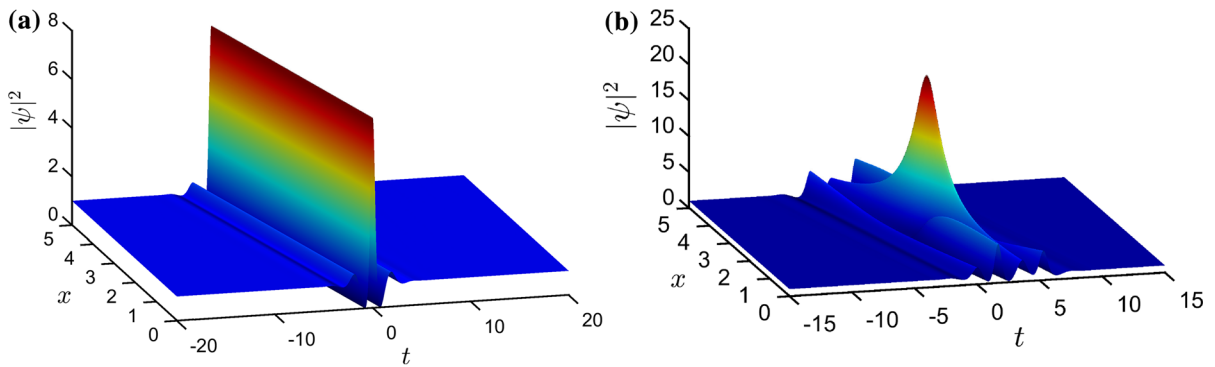


Fig. 4 Dynamically generated soliton solutions of the **a** first and **b** second order, for $\alpha = 1/8$. A breather-to-soliton conversion in Hirota equation is utilized to obtain higher-intensity solitons. Initial wave functions are extracted from the DT solutions having a plane-wave seed. The real parts of all eigen-

values satisfy Eq. (4.3). Parameters are: **a** $\lambda_1 = 1 + 0.9i$, $|\psi|_{\max}^2 = (1 + 2 \cdot 0.9)^2 = 7.84$, and **b** $\lambda_1 = 1 + 0.9i, \lambda_2 = 1 + i$, $|\psi|_{\max}^2 = (1 + 2 \cdot 0.9 + 2 \cdot 1)^2 = 23.04$, both in agreement with the PHF for breathers

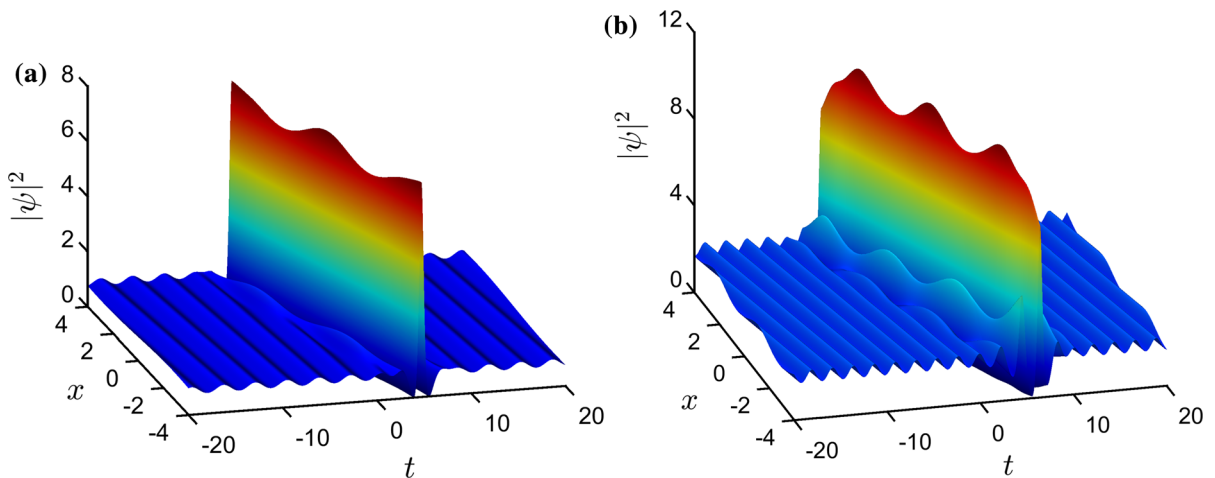


Fig. 5 Breather-to-soliton conversion of the Hirota equation on dnoidal background. Wave functions are calculated using the DT with the seed given by Eq. (3.1). Parameters are: $\alpha = 1/6, m = 0.5^2, \lambda = 0.75 + 0.9i$, with **a** $c = 1$ and **b** $c = 1.5$

longer periods and smaller amplitudes, as compared to the $c = 1.5$ case. We conclude that a weaker oscillation causes less perturbation in the soliton propagation. Therefore, the converted soliton is slightly affected, as shown in Fig. 5a, while in Fig. 5b a considerable distortion is observed.

Akhmediev breathers and Kuznetsov–Ma solitons of HE can be also produced on elliptic backgrounds. Similar to the NLSE case, ABs are produced when the imaginary part of an eigenvalue is $\nu < 1$, while the KM solitons are obtained in the $\nu > 1$ case. It was shown in [33] that the NLSE ABs are stretching out and KM

solitons are compressing, as the elliptic modulus \sqrt{m} or ν is increasing. Our calculations for Hirota equation produced the same results (not shown). Here we examine the influence of parameter c in the seed function ψ_{dn} on the period of ABs and KM solitons. We set $\alpha = 1/6, m = 0.5^2$, and $\lambda = 0.75i$ for AB, and $\alpha = 0.03, m = 0.5^2$, and $\lambda = 1.25i$ for KM soliton. When $c = 1$ (Fig. 6a), five peaks are visible, compared to seven in the $c = 1.2$ case (Fig. 6b). Results differ when the KM soliton is produced: More crests are visible for lower c , as shown in Fig. 6c, d. It is clear that a higher c

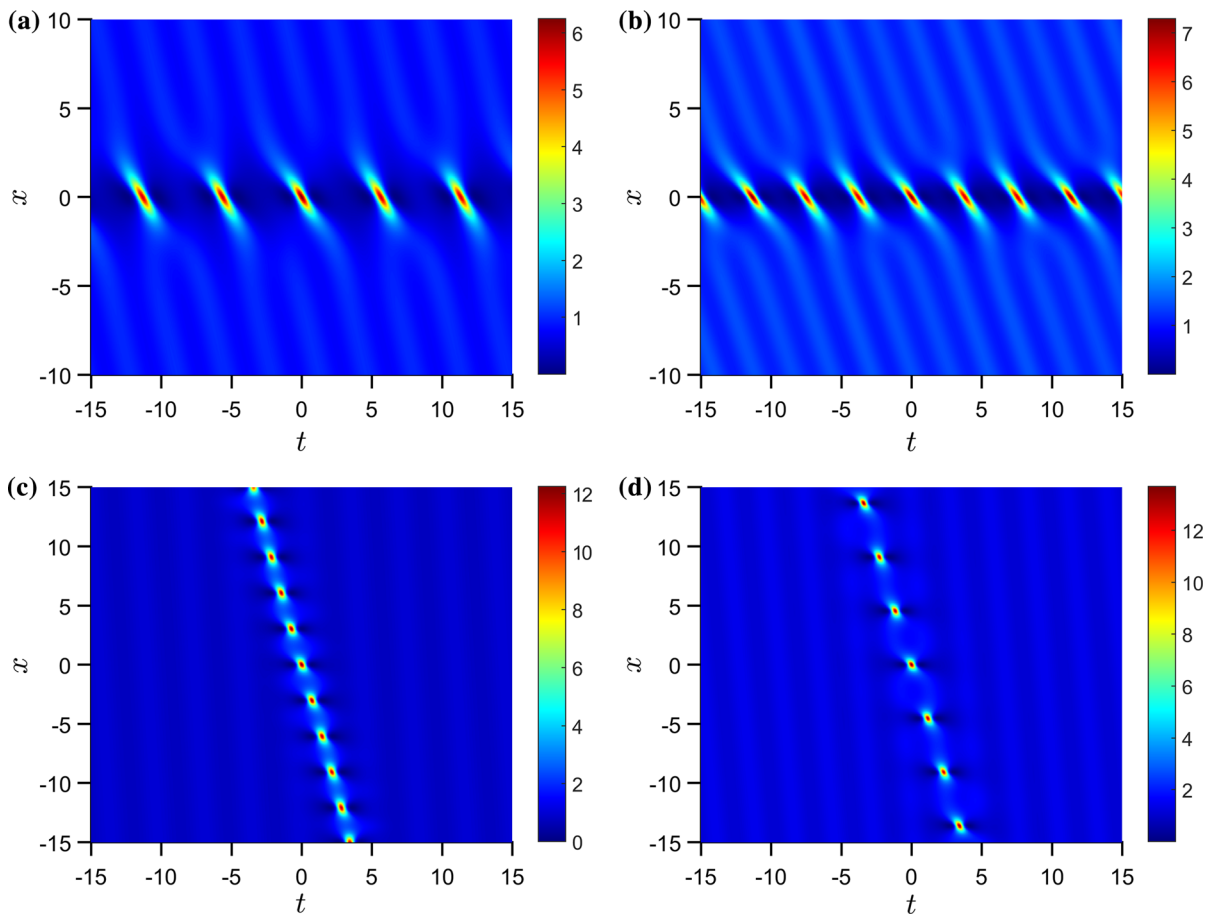


Fig. 6 First-order Akhmediev breathers obtained by the DT, with dnoidal seed from Eq. (3.1). Parameters are: $\alpha = 1/6$ and $m = 0.5^2$. The eigenvalue is $\lambda = 0.75i$, with **a** $c = 1$ and **b** $c =$

1.2. Kuznetsov–Ma soliton is obtained for $\alpha = 0.03$, $m = 0.5^2$, and $\lambda = 1.25i$, with **c** $c = 1$ and **d** $c = 1.2$

yields shorter periods of ABs and longer periods of KM solitons.

Next, we generate the first-order breathers, denoted as the dim and bright RWs, on a dnoidal background ($c = 1$). These results are similar to those in [33] and [34]. In general, the dim RW is obtained when $v \approx \frac{1}{2} - \frac{1}{2}\sqrt{1-m}$, while the bright RW is generated for $v \approx \frac{1}{2} + \frac{1}{2}\sqrt{1-m}$. In Fig. 7a, b, the dim and bright RWs are shown, respectively, for $\alpha = 0.3$ and $m = 0.5$. The intensities of dim (bright) RWs are 1.6716 (7.3284). These two RWs can be combined into a second-order solution using DT, as shown in Fig. 7c. Its intensity is always 9 (in agreement with PHF), independent of the background parametrized by m . In the special case of $m = 0.5$, the inten-

sity of this second-order rogue wave is equal to the sum of intensities of the dim and bright RWs. In this manner, we have generated a “Pythagorean triplet” of rogue waves for the Hirota equation. A comparison of these results with the same solutions of NLSE (Figs. 3, 4, and 5 in [34]) reveals a similar structure, except for the tilt introduced by the parameter α .

In Fig. 8a, b, we show the third-order breathers generated by DT for both dnoidal and cnoidal seeds. The backgrounds differ in the two cases, showing distorted oscillatory patterns. However, very sharp and strong central peaks appear similarly in both figures, suggesting that these maxima can be recognized as RWs of HE on nonuniform backgrounds.

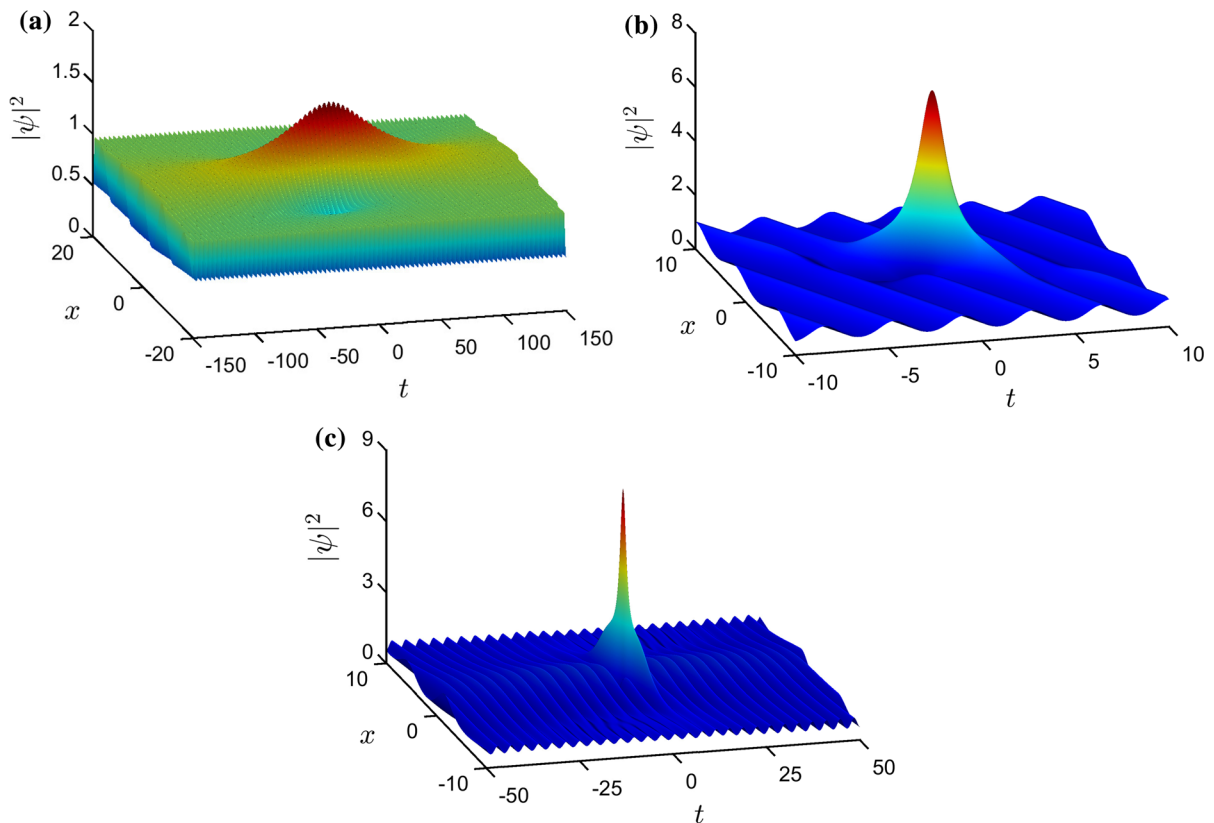


Fig. 7 **a** The dim and **b** the bright rogue waves obtained for $\alpha = 0.3$, $m = 0.5$, and $\nu \approx \frac{1}{2} \mp \frac{1}{2}\sqrt{1-m}$. **c** The second-order solution formed by the DT from RWs of **(a)** and **(b)**. The peak intensity is 9, precisely equal to the sum of its constituents' intensities

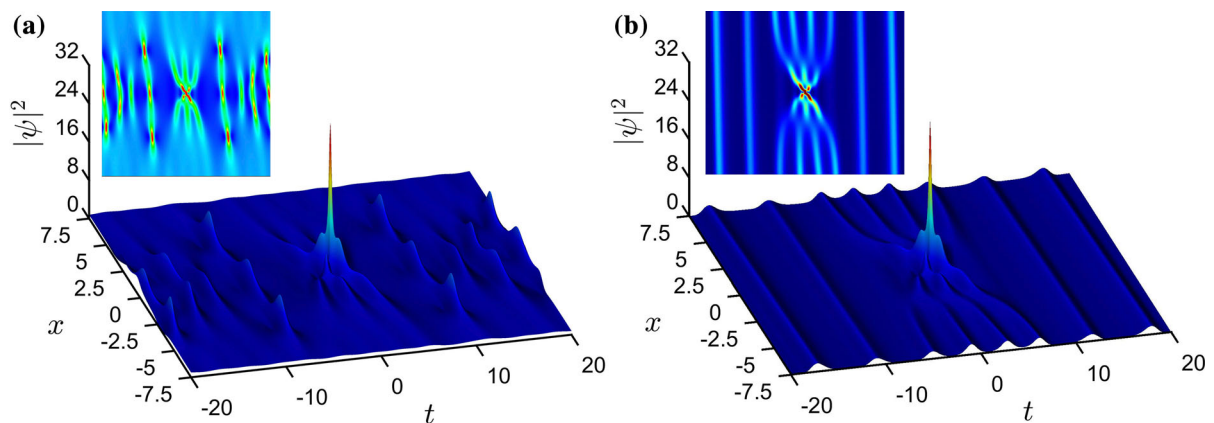


Fig. 8 Third-order breathers calculated using the DT on a nonuniform background. Parameters are $\lambda_1 = 0.91i$, $\lambda_2 = 0.81i$, $\lambda_3 = 0.61i$, and $\alpha = 0.05$. Seed functions: **a** $\psi_0 = \psi_{dn}$, $m = 1/9$, $c = 1$, and **b** $\psi_0 = \psi_{cn}$, $m = 0.98^2$, $c = \sqrt{2m-1}$. Both intensity maxima are in agreement with the PHF: **a** $|\psi|_{\max}^2 = 32.036 = [c + 2(0.91 + 0.81 + 0.61)]^2$ and

b $|\psi|_{\max}^2 = 31.810 = [c\sqrt{\frac{m}{2m-1}} + 2(0.91 + 0.81 + 0.61)]^2$. Insets in both figures show 2D intensity distributions, in order to depict strong and sharp central peaks imposed on irregular oscillatory patterns of the background

6 Conclusion

In this work, we have presented a procedure for dynamical generation of higher-order solitons and breathers of the Hirota equation on uniform background, using the Darboux transformation. Once the wave function at a particular value of the evolution variable is found using DT, it can be used as an initial condition for numerical evaluation, with appropriate boundary conditions. This dynamical evolution toward higher-order solitons and breathers is important in the situations when the existence of such solutions is questionable in the presence of modulation instability. Thus, the DT may provide analytical higher-order solutions that might not exist, owing to modulation instability, which—as a rule—exists in these solutions. We have shown that the breather-to-soliton conversion can be used to produce solitons of higher amplitude and that the periodicity of Akhmediev breathers can be utilized for dynamical generation of rogue waves.

We also presented a derivation of the Lax pair generating functions and a procedure for calculating higher-order solutions of Hirota equation when dnoidal and cnoidal JEFs are used as seed solutions for the DT. We demonstrated that higher-order ABs and Kuznetsov–Ma solitons can be generated on these nonuniform backgrounds. For particular sets of parameters, we found that the higher-order DT solutions can be treated as rogue waves of the Hirota equation.

Finally, we generalized our peak height formula for the Hirota equation, proving that the peak height of a higher-order solution is a simple linear sum of the constituent peak heights. This formula may be useful in guiding the design and production of breathers of maximal intensity in physical systems modeled by the Hirota equation.

Acknowledgements This research is supported by the Qatar National Research Fund (Projects NPRP 6-021-1-005 and NPRP 8-028-1-001), a member of the Qatar Foundation. S.N.N. acknowledges support from Grants III45016 and OI171038 of the Serbian Ministry of Education, Science and Technological Development. N.B.A. acknowledges support from Grant OI171006 of the Serbian Ministry of Education, Science and Technological Development. M.R.B. acknowledges support by the Al-Sraiya Holding Group.

7 Appendix: The general Darboux transformation scheme

A higher-order soliton (breather) solution of the N th order is a nonlinear superposition of N independent solitons (breathers), each determined by a complex eigenvalue λ_j , where $1 \leq j \leq N$ (the real part of the eigenvalue determines the angle between the localized solution and x -axis, while the imaginary part characterizes the periodic modulation frequency [27]). The N th-order wave function given by the DT is:

$$\psi_n = \psi_{n-1} + \frac{2(\lambda_n^* - \lambda_n) s_{n,1} r_{n,1}^*}{|r_{n,1}|^2 + |s_{n,1}|^2}. \tag{7.1}$$

In order to find $r_{n,1}$ and $s_{n,1}$, one has to analyze recursive relations between $r_{n,p}(x, t)$ and $s_{n,p}(x, t)$ functions of the Lax pair equations in the general form:

$$\begin{aligned} r_{n,p} = & [(\lambda_{n-1}^* - \lambda_{n-1}) s_{n-1,1}^* r_{n-1,1} s_{n-1,p+1} \\ & + (\lambda_{p+n-1} - \lambda_{n-1}) |r_{n-1,1}|^2 r_{n-1,p+1} \\ & + (\lambda_{p+n-1} - \lambda_{n-1}^*) |s_{n-1,1}|^2 r_{n-1,p+1}] \\ & / (|r_{n-1,1}|^2 + |s_{n-1,1}|^2) \\ s_{n,p} = & [(\lambda_{n-1}^* - \lambda_{n-1}) s_{n-1,1} r_{n-1,1}^* r_{n-1,p+1} \\ & + (\lambda_{p+n-1} - \lambda_{n-1}) |s_{n-1,1}|^2 s_{n-1,p+1} \\ & + (\lambda_{p+n-1} - \lambda_{n-1}^*) |r_{n-1,1}|^2 s_{n-1,p+1}] \\ & / (|r_{n-1,1}|^2 + |s_{n-1,1}|^2). \end{aligned} \tag{7.2}$$

From the last equation, it can be deduced that all $r_{n,p}$ and $s_{n,p}$ can be calculated just from $r_{1,j}$ and $s_{1,j}$, with $1 \leq j \leq N$. The functions $r_{1,j}(x, t)$ and $s_{1,j}(x, t)$, forming the Lax pair $R = \begin{pmatrix} r \\ s \end{pmatrix} \equiv \begin{pmatrix} r_{1,j} \\ s_{1,j} \end{pmatrix}$, are determined by the eigenvalue $\lambda \equiv \lambda_j$, an embedded arbitrary center of the solution (x_{0j}, t_{0j}) , and a system of linear differential equations:

$$\frac{\partial R}{\partial t} = U \cdot R, \quad \frac{\partial R}{\partial x} = V \cdot R. \tag{7.3}$$

Particularly for the Hirota equation, matrices U and V are defined as $(\psi \equiv \psi_0)$ [30]:

$$U = i \begin{bmatrix} \lambda & \psi(x, t)^* \\ \psi(x, t) & -\lambda \end{bmatrix},$$

$$V = \sum_{k=0}^3 \lambda^k \cdot i \begin{bmatrix} A_k & B_k^* \\ B_k & -A_k \end{bmatrix}, \quad (7.4)$$

where the coefficients A_k and B_k are

$$A_0 = -\frac{1}{2}|\psi|^2 - i\alpha(\psi_t^*\psi - \psi_t\psi^*),$$

$$B_0 = 2\alpha|\psi|^2\psi + \frac{1}{2}i\psi_t + \alpha\psi_{tt},$$

$$A_1 = 2\alpha|\psi|^2, \quad B_1 = \psi - 2i\alpha\psi_t$$

$$A_2 = 1, \quad B_2 = -4\alpha\psi, \quad A_3 = -4\alpha, \quad B_3 = 0. \quad (7.5)$$

References

- Hirota, R.: Exact envelope-soliton solutions of a nonlinear wave equation. *J. Math. Phys.* **14**, 805–809 (1973)
- Tao, Y., He, J.: Multisolitons, breathers, and rogue waves for the Hirota equation generated by the Darboux transformation. *Phys. Rev. E* **85**, 026601 (2012)
- Guo, R., Zhao, X.-J.: Discrete Hirota equation: discrete Darboux transformation and new discrete soliton solutions. *Nonlinear Dyn.* **84**, 1901–1907 (2016)
- Dudley, J.M., Dias, F., Erkintalo, M., Genty, G.: Instabilities, breathers and rogue waves in optics. *Nat. Photon.* **8**, 755 (2014)
- Osborne, A.S.: *Nonlinear Ocean Waves and the Inverse Scattering Transform*. Academic Press, New York (2010)
- Biswas, A., Khalique, C.M.: Stationary solutions for nonlinear dispersive Schrödinger equation. *Nonlinear Dyn.* **63**, 623–626 (2011)
- Mirzazadeh, M., Eslami, M., Zerrad, E., Mahmood, M.F., Biswas, A., Belić, M.: Optical solitons in nonlinear directional couplers by sine-cosine function method and Bernoulli's equation approach. *Nonlinear Dyn.* **81**, 1933–1349 (2015)
- Chin, S.A., Ashour, O.A., Belić, M.R.: Anatomy of the Akhmediev breather: cascading instability, first formation time, and Fermi-Pasta-Ulam recurrence. *Phys. Rev. E* **92**, 063202 (2015)
- Mani Rajan, M.S., Mahalingam, A.: Nonautonomous solitons in modified inhomogeneous Hirota equation: soliton control and soliton interaction. *Nonlinear Dyn.* **79**, 2469–2484 (2015)
- Wang, D.-S., Chen, F., Wen, X.-Y.: Darboux transformation of the general Hirota equation: multisoliton solutions, breather solutions and rogue wave solutions. *Adv. Differ. Equ.* **2016**, 67 (2016)
- Agrawal, G.P.: *Applications of Nonlinear Fiber Optics*. Academic Press, San Diego (2001)
- Guo, R., Hao, H.Q.: Breathers and multi-solitons solutions for the higher-order generalized nonlinear Schrödinger equation. *Commun. Nonlinear. Sci. Numer. Simul.* **18**, 2426–2435 (2013)
- Potasek, M.J., Tabor, M.: Exact solutions for an extended nonlinear Schrödinger equation. *Phys. Lett. A* **154**, 449 (1991)
- Cavalcanti, S.B., Cressoni, J.C., da Cruz, H.R., Gouveia-Neto, A.S.: Modulation instability in the region of minimum group-velocity dispersion of single-mode optical fibers via an extended nonlinear Schrödinger equation. *Phys. Rev. A* **43**, 6162 (1991)
- Trippenbach, M., Band, Y.B.: Effects of self-steepening and self-frequency shifting on short-pulse splitting in dispersive nonlinear media. *Phys. Rev. A* **57**, 4791 (1998)
- Anderson, D., Lisak, M.: Nonlinear asymmetric self-phase modulation and self-steepening of pulses in long optical waveguides. *Phys. Rev. A* **27**, 1393 (1983)
- Dudley, J.M., Taylor, J.M.: *Supercontinuum Generation in Optical Fibers*. Cambridge University Press, Cambridge (2010)
- Chin, S.A., Ashour, O.A., Nikolić, S.N., Belić, M.R.: Maximal intensity higher-order Akhmediev breathers of the nonlinear Schrödinger equation and their systematic generation. *Phys. Lett. A* **380**, 3625–3629 (2016)
- Ankiewicz, A., Soto-Crespo, J.M., Akhmediev, N.: Rogue waves and solutions of the Hirota equation. *Phys. Rev. E* **81**, 046602 (2010)
- Guo, B., Ling, L., Liu, Q.P.: Nonlinear Schrödinger equation: generalized Darboux transformation and rogue wave solutions. *Phys. Rev. E* **85**, 026607 (2012)
- Mu, G., Qin, Z., Chow, K.W., Ee, B.K.: Localized modes of the Hirota equation: Nth order rogue wave and a separation of variable technique. *Commun. Nonlinear Sci. Numer. Simul.* **39**, 118–133 (2016)
- Yang, Y., Yan, Z., Malomed, B.A.: Rogue waves, rational solitons, and modulational instability in an integrable fifth-order nonlinear Schrödinger equation. *Chaos* **25**, 103112 (2015)
- Akhmediev, N., Ankiewicz, A., Soto-Crespo, J.M.: Rogue waves and rational solutions of the nonlinear Schrödinger equation. *Phys. Rev. E* **80**, 026601 (2009)
- Kedziora, D.J., Ankiewicz, A., Akhmediev, N.: Circular rogue wave clusters. *Phys. Rev. E* **84**, 056611 (2011)
- Kedziora, D.J., Ankiewicz, A., Akhmediev, N.: Triangular rogue wave clusters. *Phys. Rev. E* **86**, 056602 (2012)
- Akhmediev, N., et al.: Roadmap on optical rogue waves and extreme events. *J. Opt.* **18**, 063001 (2016)
- Akhmediev, N., Soto-Crespo, J.M., Ankiewicz, A.: Extreme waves that appear from nowhere: on the nature of rogue waves. *Phys. Lett. A* **373**, 2137–2145 (2009)
- Akhmediev, N., Eleonskii, V.M., Kulagin, N.E.: N-modulation signals in a single-mode optical waveguide under nonlinear conditions. *Zh. Eksp. Teor. Fiz.* **94**, 159–170 (1988). [*Sov. Phys. JETP* **67**, 89-95 (1988)]
- Geng, X.G., Lv, Y.Y.: Darboux transformation for an integrable generalization of the nonlinear Schrödinger equation. *Nonlinear Dyn.* **69**, 1621–1630 (2012)
- Chowdury, A., Ankiewicz, A., Akhmediev, N.: Moving breathers and breather-to-soliton conversion for the Hirota equation. *Proc. R. Soc. A* **471**, 20150130 (2015)
- Chowdury, A., Kedziora, D.J., Ankiewicz, A., Akhmediev, N.: Breather-to-soliton conversions described by the quintic equation of the nonlinear Schrödinger hierarchy. *Phys. Rev. E* **91**, 032928 (2015)

32. Schwalm, W.A.: Lectures on Selected Topics in Mathematical Physics: Elliptic Function-and Elliptic Integrals, vol. 68. Morgan & Claypool publication as part of IOP Concise Physics, San Rafael (2015)
33. Kedziora, D.J., Ankiewicz, A., Akhmediev, N.: Rogue waves and solitons on a cnoidal background. *Eur. Phys. J. Spec. Top.* **223**, 43–62 (2014)
34. Chin, S.A., Ashour, O.A., Nikolić, S.N., Belić, M.R.: Peak-height formula for higher-order breathers of the nonlinear Schrödinger equation on nonuniform backgrounds. *Phys. Rev. E* **95**, 012211 (2017)
35. Ankiewicz, A., Kedziora, D.J., Chowdury, A., Bandelow, U., Akhmediev, N.: Infinite hierarchy of nonlinear Schrödinger equations and their solutions. *Phys. Rev. E* **93**, 012206 (2016)
36. Kedziora, D.J., Ankiewicz, A., Chowdury, A., Akhmediev, N.: Integrable equations of the infinite nonlinear Schrödinger equation hierarchy with time variable coefficients. *Chaos* **25**, 103114 (2015)
37. Ankiewicz, A., Wang, Y., Wabnitz, S., Akhmediev, N.: Extended nonlinear Schrödinger equation with higher-order odd and even terms and its rogue wave solutions. *Phys. Rev. E* **89**, 012907 (2014)
38. Yang, Y., Wang, X., Yan, Z.: Optical temporal rogue waves in the generalized inhomogeneous nonlinear Schrödinger equation with varying higher-order even and odd terms. *Nonlinear Dyn.* **81**, 833–842 (2015)